Submergence and Uplift of Settlements in the Area of Helike, Greece, from the Early Bronze Age to Late Antiquity

Article *in* Geoarchaeology · July 2011

DOI: 10.1002/gea.20366

CITATIONS
42

READS
242

2 authors:

Steven Soter
American Museum of Natural History
65 PUBLICATIONS **3,377** CITATIONS

SEE PROFILE

Dora Katsonopoulou
The Institute for Archaeology of Paros and the Cyclades
60 PUBLICATIONS **307** CITATIONS

SEE PROFILE

Submergence and Uplift of Settlements in the Area of Helike, Greece, from the Early Bronze Age to Late Antiquity

Steven Soter[1,*] and Dora Katsonopoulou[2]

[1]*Environmental Studies Program, New York University, and American Museum of Natural History, Central Park West at 79th Street, New York, NY 10024*
[2]*The Helike Project and The Helike Society, 58 Solomou Street, Athens 106 82, Greece*

Excavations in the Helike Delta on the Gulf of Corinth have brought to light architectural remains from the Early Bronze Age (EBA), Geometric, Classical, Hellenistic, Roman, and Byzantine periods. Borehole results suggest that a lagoon intermittently occupied much of the delta during the Holocene. We discovered a well-preserved EBA settlement about 1 km inland from the present shore, buried under 3 to 5 m of fine sediments containing marine, brackish, and freshwater microfossils. A Classical site 130 m away, buried under 3 m of similar sediments, may have been destroyed by the earthquake and tsunami of 373 B.C., which submerged the city of Helike. Possible tsunami evidence is noted. Although the EBA and Classical sites were both long submerged and buried by lagoonal sediments, tectonic uplift has raised both horizons above sea level. A shallow black clay layer suggests that a marsh covered the Classical and EBA sites in Byzantine times. © 2011 Wiley Periodicals, Inc.

INTRODUCTION

On the southwest shore of the Gulf of Corinth, deposits from three rivers have coalesced to form a broad delta plain (Figure 1). Here, in 373 B.C., an earthquake and tsunami destroyed and submerged Helike, the foremost city of Achaea in the northern Peloponnesos. Anderson (1954) and Katsonopoulou (2002) review the topography and archaeology of Achaea. The principal sources for the destruction of Helike are Pausanias (7.24.6 and 7.24.12), Strabo (8.7.2), Diodoros (15.48), and Aelian (*Hist. Animal.* 11.19). For all available ancient sources on the earthquake, see Katsonopoulou (2005a). In A.D. 172/173, Pausanias visited the site of Helike, about 7.5 km southeast of Aigion, and reported that the drowned ruins were still visible but much corroded by saltwater. Later, all traces of Helike were lost (Marinatos, 1960; Papadopoulos, 1998; Soter & Katsonopoulou, 1999; Katsonopoulou, 2005a).

The Helike Project began to search for the site in 1988, surveying 8 km^2 of seafloor with sidescan and subbottom sonar. The survey showed no clear evidence of a

*Corresponding author; E-mail: soter@amnh.org.

Geoarchaeology: An International Journal, Vol. 26, No. 4, 584–610 (2011)

Published online in Wiley Online Library (wileyonlinelibrary.com). DOI:10.1002/gea.20366

Figure 1. Aerial view of the Helike Delta, looking southeast. The delta plain lies between the Gulf of Corinth (left) and the mountains of the Peloponnesos (right). Three rivers, with artificial embankments, cross the delta: the Selinous (foreground), Kerynites (midground), and Vouraikos (background). The Helike Fault marks the sharp contact between the mountains (footwall) and the plain (hanging wall). Photo by Ian Hay, May 2001, for the Helike Project.

city on or under the seafloor, so we shifted the search to the adjacent coastal plain (Soter & Katsonopoulou, 1998, 1999). Katsonopoulou (1995) found evidence in the ancient sources suggesting that Helike was submerged in a lagoon, not in the sea. From 1991 to 2002, we drilled 99 boreholes on the delta, and found pottery fragments and other evidence of occupation within an area of about 2 km^2. The occupation horizons ranged in depth from about 14 m to near the surface, and in age from Neolithic to Late Byzantine times.

Since 2000, the Helike Project has conducted annual excavations in the delta between the rivers Selinous and Kerynites, and has brought to light sites dating from the Early Bronze Age (EBA), Mycenaean, Geometric, Classical, Hellenistic, Roman, and Late Byzantine periods (Katsonopoulou, 2002, 2005b, 2007, 2011b).

Soter and Katsonopoulou (1999) describe the geological setting of the search for Helike, while Soter et al. (2001) and Alvarez-Zarikian, Soter, and Katsonopoulou (2008) provide the paleoenvironmental data based on microfauna in sediment samples from boreholes and trenches. This paper focuses on the geological evolution of the Helike delta in the light of archaeology, and aims to synthesize and interpret the principal results derived from boreholes and archaeological excavations.

The Gulf of Corinth occupies a rift valley in the most seismically active part of Europe. The southern margin of the Gulf is bounded by a series of normal faults

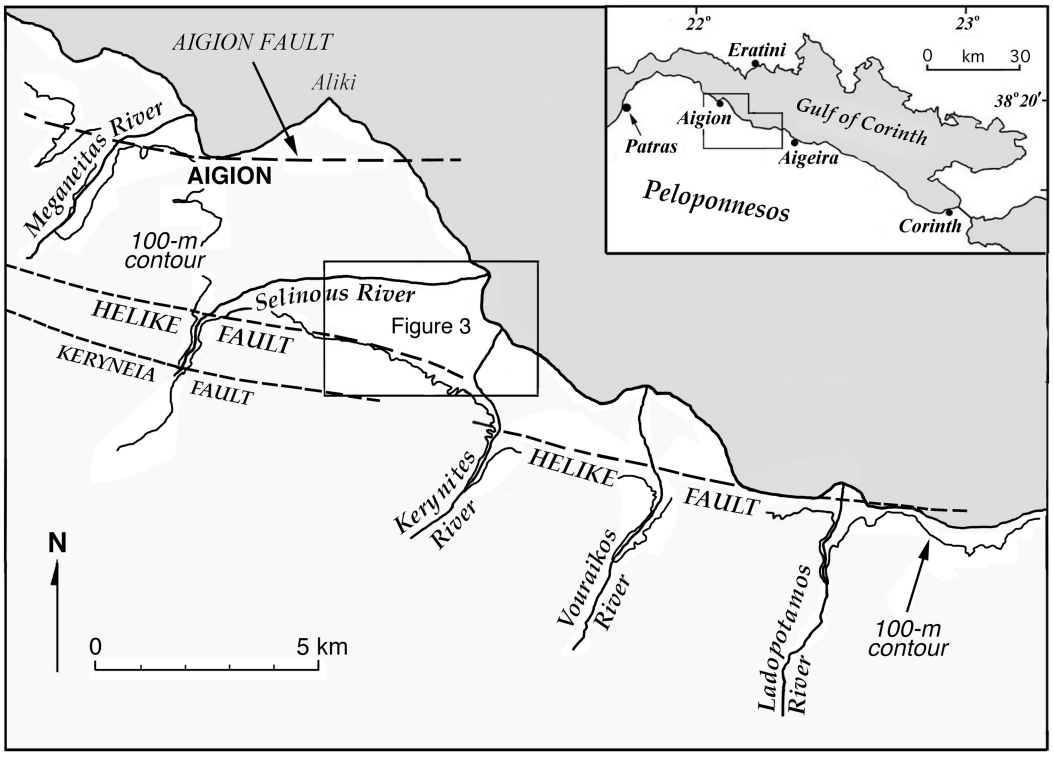

Figure 2. Chart of Aigialeia, showing the Helike Fault. The boreholes and excavations are in the central rectangle, as detailed in Figure 3.

dipping northward. Prominent among them is the Helike Fault, which separates the delta plain on the hanging wall block from the mountains on the footwall block to the south (Figure 2). Earthquakes on the Helike Fault result in uplift of the inland footwall block and subsidence of the coastal hanging wall block (Soter, 1998; Soter & Katsonopoulou, 1999).

The last major earthquake on the Helike Fault, in 1861, produced a scarp 13 to 15 km long at the contact between the delta plain and the mountains. The earthquake triggered intense soil liquefaction, and the delta subsided by 1–2 m, drowning a coastal strip 13 km long and up to 200 m wide (Schmidt, 1875; Koukouvelas et al., 2001). Scaling relationships based on the length of the surface rupture suggest that the 1861 earthquake had a moment magnitude of 6 to 7 and a fault displacement of less than 2 m (Wells & Coppersmith, 1994; Papadopoulos, Vassilopoulou, & Plessa, 2000).

Dating of elevated fossil shorelines exposed on the rocky footwall southeast of the delta (Mouyaris, Papastamatiou, & Vita-Finzi, 1992; Stewart & Vita-Finzi, 1996; Pirazzoli et al. 2004) suggests that the footwall block has risen at a average rate of about 2.4 m per kyr during the Holocene (Soter, 1998). The uplift has been gradual as well as episodic, punctuated by abrupt seismic events. The fossil shoreline data suggest that about 2 m of footwall uplift occurred between 450 B.C. and A.D. 150 (Soter, 1998). The earthquake of 373 B.C. may have contributed to that episode, together with an increased rate of aseismic slip.

According to Diodoros, the earthquake struck at night and the tsunami arrived with daylight. This suggests a time lag of a few hours. The initial shock may have caused ground liquefaction and mass sliding, leading to subsidence and flooding of the delta (Leonards, Sotiropoulos, & Kavvadas, 1988). One or more strong aftershocks on the weakened delta could have triggered a massive submarine landslide, which produced the tsunami (Soter & Katsonopoulou, 1999).

Pausanias recorded that only the tops of the trees in the sacred grove of Poseidon remained visible above water after the submergence of Helike. The sanctuary was undoubtedly of great antiquity and the grove would have contained mature trees. Allowing 1 m of surface elevation at the grove before the earthquake suggests a total subsidence of at least 3 m. Since that exceeds the maximum expected tectonic displacement for an earthquake along the known length of the Helike Fault, sedimentary flow failure probably contributed to the subsidence.

Ferentinos and Papatheodorou (2005) hypothesized that the earthquake triggered a landslide on the surface of the delta; at the head of the landslide, the detachment of the sliding mass opened a broad and deep trench; the sea then invaded the depression, flooding the site of Helike. Whatever the exact sequence of events in 373 B.C., it appears that the delta has continued its uplift by aseismic tectonic deformation and perhaps by earthquakes on submerged faults to the north of the Helike Fault (Soter, 1998). Earthquakes have also altered the course of the rivers on the delta (Soter & Katsonopoulou, 1999; Pavlides et al., 2004).

The standard source for surface elevations in the region is the 1:5000 Greek military map, based on aerial photogrammetry from 1966. However, recent surveys (beginning with one by K. Dimitropoulos, pers. comm., 2002) have found that surface elevations in the delta area west of the Kerynites River are now lower than shown on the map by as much as 2.5 m. The cause of this discrepancy is unknown. If due to actual subsidence, the rate would be very large. In any case, for consistency we will retain the military map data in this paper and use it to define "nominal" surface elevations.

BOREHOLES AND TRENCHES

The Helike Project drilled 99 boreholes in an area of several square kilometers in the delta, with the main goal of finding ancient occupation horizons. The drilling depth ranged from 7 to 51 m, with an average of 16 m. We recovered sediment cores using a rotary drill barrel of average internal diameter 10 cm. Figure 3 shows locations of the boreholes (labeled by numbers) drilled in the central search area, together with major archaeological sites discovered through 2008. The open circles indicate boreholes that contained no traces of ceramics. The circled dots show boreholes where we found ceramic fragments in coarse sediments (gravel, etc.). We refer to such cases as "ceramic presence" because many of those ceramics may be from flood deposits rather than *in situ*. The solid circles show boreholes that penetrated one or more occupation horizons, which we recognized by the presence of ceramic fragments in fine sediments (clay, silt, sand), sometimes with burned pottery fragments, burned bone, and organic material.

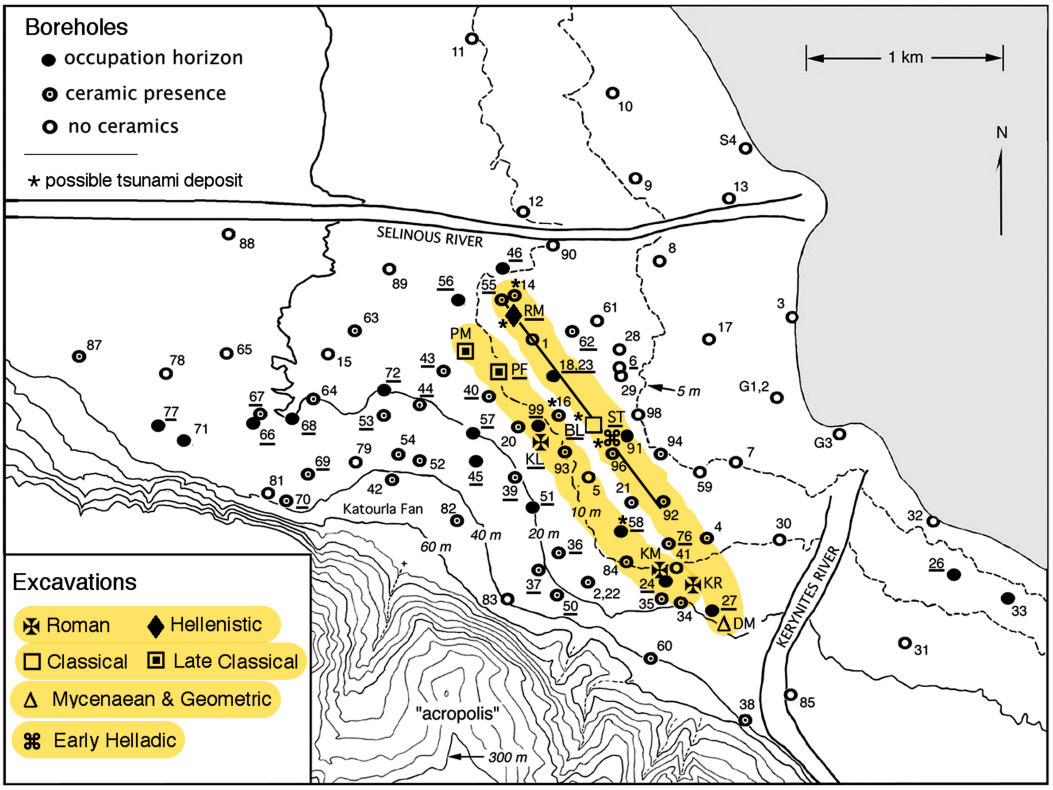

Figure 3. Topographic map of the central Helike area, showing locations of boreholes (numbered circles), excavations (lettered symbols), and the Roman road (straight line). Underlined numbers and letters indicate boreholes and excavations with vertical profiles included in Figure 4. Elevation contours are given every 20 m, plus those at 5 and 10 m above sea level, from the 1:5000 Greek military map (ca. 1966, nominal elevation data). The terms "occupation horizon" and "ceramic presence" are defined in the text. The symbol for each excavation site identifies the prevalent archaeological period there, but most trenches also contain horizons from other periods. The term "Classical" here refers mainly to the 5th century B.C. (from ca. 480 B.C. to 400 B.C.) and "Late Classical" to the 4th century (from ca. 400 B.C. to the death of Alexander in 323 B.C.).

We found no occupation horizons in boreholes drilled within 800 m of the present shore between the Selinous and Kerynites Rivers. The delta surface in this area has evidently been deposited since antiquity. The ancient shoreline would then be located near the nominal 5-m elevation contour.

Sediments from the stream valley west of the "acropolis hill" of Agios Georgios produced the Katourla Fan, a small terrestrial delta adjacent to the Helike Fault. Most of the boreholes that yielded evidence of occupied sites are concentrated around the lower periphery of the Katourla Fan, where it merges with the broad marine delta plain.

Based on excavations through 2008, the Helike Project identified nine areas of archaeological interest, here designated (in order of discovery) as the Klonis (KL), Romanos (RM), Karelis (KR), Saitis (ST), Papafilippou (PF), Balalas (BL), Komnenos (KM), Papamichalopoulou (PM), and Dimopoulou (DM) sites. We indicate these sites in Figure 3 and elsewhere by the abbreviations shown here in parentheses. Table I

Table I. Main archaeological areas.

No.	Location	Description
Klonis (KL)		E = 12.3 m
	38°13.030'N 22°07.942'E	Late Roman building, standing walls 1.5–3.6 m, pottery, clay lamps, glass fragments, clay and metallic objects, bronze coins. Classical black-glazed, Protogeometric, and Mycenaean potsherds 2.0–3.3 m.
Romanos (RM)		E = 8.8 m
B73	38°13.348'N 22°07.863'E	Occupation horizons at 2.1 and 2.65–3.15 m.
H1	Same as B73*	Hellenistic wall and associated pottery at 2.5 m, possible tsunami deposit at 3.85 m.
H3	45 m NW of B73	Late Byzantine house at 0.7 m, Roman road at 1.65 m.
H4	55 m SSW of B73	Late Byzantine cemetery at 1.1–1.25 m, pair of bronze earrings.
H12	6 m E of H1	Roman road at 1.65 m, Hellenistic wall and pottery at 2.2 m.
	Rectangular area 39 × 25 m centered at ~38°13.330'N, 22°7.895'E	*Well-preserved remains of a major dye-works, with four pebbled floor cisterns, vats and other structures for washing and dyeing fabrics, habitation rooms, storage, and workshop areas at 2.3 m, black-glazed, red-glazed, West Slope, and relief decorated vases, a terra-cotta Tanagra lady, clay lamps, loom weights, metal objects in bronze, iron and lead, numerous bronze coins.*
Karelis (KR)		E = 18 m
H5	38°12.620'N 22°08.470'E	Group of five tile-covered Early Roman graves, clay vases and lamps, bronze coin at 1.2–2.0 m.
Saitis (ST)		E = 5.8 m
B75	17 m E of H21	Occupation horizons at 2.0, 3.0, 5.2–6.6 (burned ceramics and bone), and 7.5 m.
B91	50 m NE of H21	Occupation horizons at 3.6, 4.4, and 5.7 m.
H7	5 m SE of H21	Early Helladic III buildings and associated pottery at 3.3–3.6 m.
H8	34 m SSW of H21	Classical and Archaic pottery layers at 2.45–3.0 m.
H21	38°13.037'N 22°08.190′E	Roman road at 1.8 m, Early Helladic III buildings and complete pottery at 3.3–3.6 m.
H22	23 m N of H21	EH III–II buildings and pottery at 3.3–4.1 m, a rare *depas amphikypellon* cup and items in gold and silver.
H26	*See Fig. 10*	*EH III buildings and associated pottery at 3.0–3.8 m.*
H38	*See Fig. 10*	*EH III–II buildings including part of a corridor house and complete pottery at 3.8–4.5 m, clay spindle, bone tools.*
H43	*See Fig. 10*	*EH III–II buildings and cobbled street 3.9–4.5 m, abundant complete and decorated pottery, pithoi, 3 clay spools, bone and stone tools.*
H51	*See Fig. 10*	*EH III–II buildings at 3.45–4.5 m, rich pottery including complete vases, pithoi, bone and stone tools, obsidian blades, flint arrowhead.*

H61	*See Fig. 10*	*EH III–II buildings preserving pebble floors at 3.1–4.5 m, abundant pottery and complete cups, clay spindle, bone and stone tools, obsidian blades, and flint-chipped stone.*
Papafilippou (PF)		E = 10.3 m
H9	38°13.210′N 22°07.807′E	Late Classical/Early Hellenistic destruction layer (ca. 330–300 B.C.) of roof tiles, pottery, and bronze coins at 2.6–2.9 m.
H11, H35	*Same area*	*Late Classical/Early Hellenistic destruction layer (ca. 330–300 B.C.) of roof tiles, with plain, black-glazed and decorated pottery, clay loom weights, and bronze coins at average depth 2.0–2.6 m.*
H29	*Same area*	*Part of a well-built stone wall at 2.1 m, Late Classical/Early Hellenistic destruction layer (ca. 330–300 B.C.) of roof tiles; plain, black-glazed, and decorated pottery; bronze coin; and clay loom weights at 1.6–2.4 m.*
Balalas (BL)		E = 6.0 m
H10	10 m NE of H18	Remains of Hellenistic structure and associated potsherds in black clay layer at 2.1–2.2 m depth, Classical potsherds at 3.7–3.9 m.
H18	38°13.095′N 22°08.129′E	Roman road at 2.3 m, destroyed Hellenistic and Classical walls and associated potsherds at about 3.0 and 3.4 m.
H19	24 m S of H18	Classical walls with associated pottery and coins at 3.0–3.4 m, silver coin of Sikyon at 2.9 m, bronze coin of Aigina at 3.15 m, Archaic clay female idol at 3.4 m.
Komnenos (KM)		E = 10 to 12 m
H13	*5 m N of H16*	*Destroyed Roman building with pebbled floors at 0.3–0.5 m.*
H14	*38°12.677′N 22°08.377′E*	*Roman storage areas at 0.3 m and cistern with pebbled/tile floor at 1.9 m, human skeleton at ca 1.0 m crushed by destruction layer of roof tiles and clay plinths.*
H16	*50 m NNW of H14*	*Roman buildings with large pithoi and pottery at 0.3 m.*
Papamichalopoulou (PM)		E = 11.5 m
H25 H33	*38°13.250′N 22°07.687′E*	*Roman destruction layer of scattered wall stones, roof tiles, and pottery at 1.1–1.2 m. Group of seven Late Classical/Early Hellenistic tile-covered graves at 1.9 m, one bronze ring.*
Dimopoulou (DM)		E = 18.0 m
H58	*38°12.543′N 22°08.571′E*	*Group of seven Roman tile-covered graves with clay and glass vases, one bronze coin of Konstantine the Great, objects of bronze, bone, and iron at 1.3–2.0 m. Geometric and Mycenaean pottery layers at 2.1–2.3 and 3.8–4.1 m, respectively.*
H59	*15 m W of H58*	*Geometric and Proto-Geometric pottery at 2–3 m, circular hearth at 2.1 m.*

* This was the only trench coinciding with a borehole.
B = borehole number, H = trench number, E = nominal surface elevation above sea level ca. 1966.
Trenches described in *italics* were not previously published.

gives the locations and archaeological data for selected boreholes and trenches in these nine areas.

In addition, we discovered a major Roman road, which intersects trenches in the Romanos, Balalas, and Saitis sites. The road is 5–6 m wide, 0.7 m thick, and consists of three layers, made of cobbles, gravel, and packed soil. The road was excavated in nine trenches, which allowed us to trace its straight course for 800 m (Katsonopoulou, 2002, 2011a). Tsokas et al. (2009) detected the road with electrical tomography and extended its known length to 1300 m, as shown by the straight line in Figure 3. The trenches ranged in area from ca. 30 to 80 m^2, except for the extensive dye-works site in RM, which was ca. 975 m^2.

Klonis (KL)

The Helike Project opened two 4-m squares in this area in 1995 to investigate a magnetic geophysical anomaly (Soter & Katsonopoulou, 1999). Excavation revealed a large Roman building with walls standing 2 m high constructed with successive layers of unworked stone, baked bricks, and mortar as binding material. In addition to large quantities of pottery, the finds included fragments from glass vases, objects of bone and bronze, and fragments of marble decoration in *opus sectile*. Bronze coins dating from the time of Emperor Aurelian (A.D. 270–275) to the late 4th to early 5th century A.D. provide evidence for the lifespan of the building. An extensive destruction layer both within and outside the building shows that an earthquake destroyed the building, probably in the late 5th century (Katsonopoulou, 1998; Koukouvelas et al., 2001, 2005). This is significant because we have not found any historical documentation for an earthquake in this area in late Roman times. The deeper excavation strata also yielded a group of Classical, Protogeometric, and Mycenaean potsherds. These were not found *in situ* and probably originated from a horizon below or near the Roman building.

Romanos (RM)

Our georadar survey in this area in 1996 detected a target of interest at 2.4 m depth (Kutrubes et al., 2003). In 1998, we drilled borehole B73 on the spot to a depth of 9.3 m. Sediment cores contained ceramic-bearing horizons at 2.1, 2.9, and 4.7 m below ground. We opened trench H1 at the identical spot in 2000, followed later by other trenches nearby. Trench H1 revealed a well-built wall at ca. 2.4 m depth, dated to the Hellenistic period (3rd/2nd century B.C.) based on associated finds. The Hellenistic wall continued in the adjacent trenches H12 and H23, which also revealed parts of a Roman road directed NW to SE, at a depth of 1.65 m. In trench H3, about 50 m northwest of H12, the Roman road continued at the same depth, below a Late Byzantine house at 0.7 m. We also found the road in trench H42, located midway between H3 and H12. Associated coins from the surface of the road and architectural remains above and below date the road to the Roman period.

Excavation of a series of trenches about 50 m southeast of H12 revealed at ca. 2.3 m depth the well-preserved remains of a major dye-works building, including a

complex of four pebbled floor cisterns with surrounding vats and other structures for washing and dyeing fabrics, habitation rooms, storage, and workshop areas (Katsonopoulou, 2010). Associated finds include a large array of Early to Middle Hellenistic pottery (black-glazed, red-glazed, West Slope, and relief decorated vases), a terra-cotta Tanagra lady, clay lamps and loom weights, many metal objects in bronze, iron and lead, and a rich collection of bronze coins.

Karelis (KR)

Trench H5 was opened in 2000 to investigate a strong georadar anomaly found in a vineyard (Kutrubes et al., 2003). Excavation revealed a group of five tile-covered tombs containing grave goods dated to the 2nd to 3rd centuries AD (Katsonopoulou, 2005b) about 1.5 m below the surface. The massive tiles covering the tombs produced the strong radar reflections.

Saitis (ST)

We first examined this area in 1998 by drilling borehole B75 to a depth of 11 m. The core samples revealed ancient pottery between 3 and 5.2 m depth, followed by a rich concentration of burned pottery, bone, and charcoal from 5.2 to 6.6 m. Charcoal at 6.4 m gave a calibrated radiocarbon age of 4400 ± 120 B.P. (Table II). This promising site was investigated by excavating eight trenches, from 2000 to 2007 (H7, H21, H22, H26, H38, H43, H51, and H61). All of them revealed architectural remains of

Table II. Radiocarbon dates.

No.	d(m)	h(m)	Description	$\delta^{13}C$	^{14}C Age B.P.	Cal. Age B.P.	Lab. No.
B71:17	5.30	19.0	Charcoal	−22.97	1610 ± 35	1470 ± 60	OS-22964
B75:10	6.40	−0.6	Charcoal	−27.6	3950 ± 50	4400 ± 120	Beta 125829
B56:24	7.60	3.4	Carbon	−26.51	7660 ± 100	8900 ± 100	OS-24804
B58:14	8.25	0.25	Carbon	−24.9	5640 ± 50	6410 ± 100	Beta 125826
B72:27	10.20	8.8	Carbon	−26.8	2950 ± 40	3100 ± 150	Beta 125828
B61:16	10.40	−3.9	Wood	−26.24	5460 ± 35	6250 ± 40	OS-22219
B70:45	12.60	10.9	Charcoal	−22.24	525 ± 40	520 ± 40	OS-22237
B68:44	12.65	8.35	Charcoal	−21.79	6160 ± 85	7040 ± 140	OS-23504
B58:16	13.65	−5.15	Charcoal	−25.99	5080 ± 55	5830 ± 80	OS-22694
B72:35	13.90	5.1	Carbon	−26.02	5740 ± 390	6610 ± 430	OS-23505
B61:21	17.55	−11.05	Seagrass fibers	−17.72	5840 ± 50	5825 ± 65	OS-22236
B4:16	38.50	−30.5	Sediment	−27.28	7490 ± 40	8360 ± 150	OS-11490

Notes: No. = borehole:sample number, d(m) = depth in meters below surface, h(m) = elevation in meters relative to sea level, Beta = Beta Analytic, OS = Woods Hole AMS.
In calibrating the marine sample B61:21, we used a correction factor of $\Delta R = 380$ yr for the Gulf of Corinth to augment the normal marine reservoir effect, as discussed by Soter (1998).

rectangular buildings belonging to a well-preserved Early Bronze Age (EBA) coastal settlement dating from the Early Helladic II–III periods, ca. 2500–2200 B.C. (Katsonopoulou, 2002, 2005b, 2007, 2011b). The buildings, including part of a "corridor house," are made of cobbled stones of varied colors. They preserve their contents intact, including abundant pottery, bone and stone tools, clay objects related to textile manufacture, obsidian blades, flint objects, and small items in gold and silver. The numerous complete vases from the rooms excavated so far include rare shapes of Anatolian origin and a drinking cup of Trojan shape, a *depas amphikypellon* (Katsarou-Tzeveleki, in press; Katsonopoulou, 2011b). Trench H21 also exposed the Roman road at about 1.8 m. Trench H8, located 40 m southwest (inland) of H7, contained no architectural remains but yielded numerous Classical and Archaic potsherds.

Papafilippou (PF)

Trench H9 was opened in 2000, followed by three adjacent trenches (H11, H29, and H35) in later years (Katsonopoulou, 2005b). All trenches revealed a thick destruction layer at about 2.0 m depth, containing a large number of plain and painted roof tiles and potsherds from plain, black-glazed, and red-figured decorated vases, clay loom weights, and two bronze coins dating from the late 4th to early 3rd centuries B.C. (after the historic earthquake). Under the destruction layer in trench H29, part of a well-built stone wall was found at 2.1 m.

Balalas (BL)

Trench H10 was opened in 2000 in the Balalas area, about 130 m northwest of the Saitis area. Remains of scattered wall stones were found within a thick stratum of fine black clay about 2.1–2.2 m below the surface. Trench H18, opened in 2001 about 10 m southwest of H10, revealed the Roman road at 2.3 m depth, and the remains of walls at 2.9 and 3.15–3.4 m, dated on the basis of associated pottery to Hellenistic and Classical times, respectively. A test borehole within H18 recovered a Classical black-glazed ceramic fragment from about 3.5 m. Trench H19, opened 24 m south of H18 in the same field (also in 2001), revealed the corner walls of a building at 3.0–3.4 m depth. Associated pottery included Classical potsherds of drinking and eating vessels, storage, and transport vases. Among the finds were a bronze coin of Aigina (early 4th century B.C.) and a silver coin of Sikyon with an image of wreathed Apollo (ca. 340–330 B.C.), the terra-cotta head of an Archaic female painted idol, and a small clay mask shaped like the head of a Silenus (Katsonopoulou, 2002). Test excavations opened landward and within 150 m of the BL site did not reveal any structures.

Komnenos (KM)

The Helike Project opened trenches H13, H14, and H16 in 2001 to investigate a strong georadar target found in 1996 (Kutrubes et al., 2003) under a local road. Excavation (supervised by R. Stieglitz) brought to light architectural remains of large

Roman buildings and an extensive commercial establishment, including a rectangular storage tank with a pebble/tile floor 2 m deep. A human skeleton was found crushed under fallen debris on the steps descending into the tank, possible evidence of an earthquake in Roman times.

Papamichalopoulou (PM)

Two trenches were opened in 2002 and 2003 about 200 m northwest of the PF area. We discovered a Roman destruction layer of wall stones, roof tiles, pottery, fragments of glass vases, and metal objects including a complete iron door key at 1.1 m depth. In a horizon at 1.9 m, under the Roman remains, we found seven well-constructed tile-covered graves of the late 4th to early 3rd centuries B.C., with burials in good state of preservation. One of the graves, with the skeleton of an adult male, contained a bronze ring.

Dimopoulou (DM)

The Helike Project opened trench H58 in 2006 near the Kerynites River in Nikolaiika. At 1.3–2.0 m, the excavations brought to light a group of seven Roman tile-covered tombs containing rich grave goods, including many clay and glass vases, a bronze coin of Konstantine the Great, iron knives, and luxury objects of bronze and ivory. Excavation of deeper archaeological horizons revealed fine pottery of the Geometric and Mycenaean periods, at 2.1–2.3 and 3.8–4.1 m, respectively. Excavation of trench H59 in the same area in 2007 brought to light Geometric pottery and a circular hearth at 2–3 m.

AGE–DEPTH PROFILES

Figure 4 shows schematic profiles of boreholes and trenches where occupation horizons were found, arranged in rank order of decreasing nominal surface elevation above mean sea level. The numbers alongside some of the profiles give the ages of dated samples in centuries B.P. The occupation horizons range in depth from near the surface down to about 14 m below the surface, and in age from the Late Byzantine to Late Neolithic periods. Most of them are above present sea level. Many boreholes contained multiple occupation horizons, and some occupation horizons included charred material (ceramics, bones, or blackened stones).

Figure 5 plots the age versus depth of the dated samples. Diagnostic ceramics come from excavated trenches. Table I summarizes the data for those archaeological horizons. We also dated selected samples from boreholes using radiocarbon for organic material and optical luminescence for non-diagnostic ceramic fragments. Soter and Katsonopoulou (1999) tabulated the ages of such samples acquired prior to 1998, and Table II in this paper lists radiocarbon dates for samples acquired more recently. Some of the scatter in radiocarbon dates is probably due to the mobilization and redeposition of sediments containing old carbon, a common problem in high-energy delta environments (Stanley & Hait, 2000). Because most boreholes

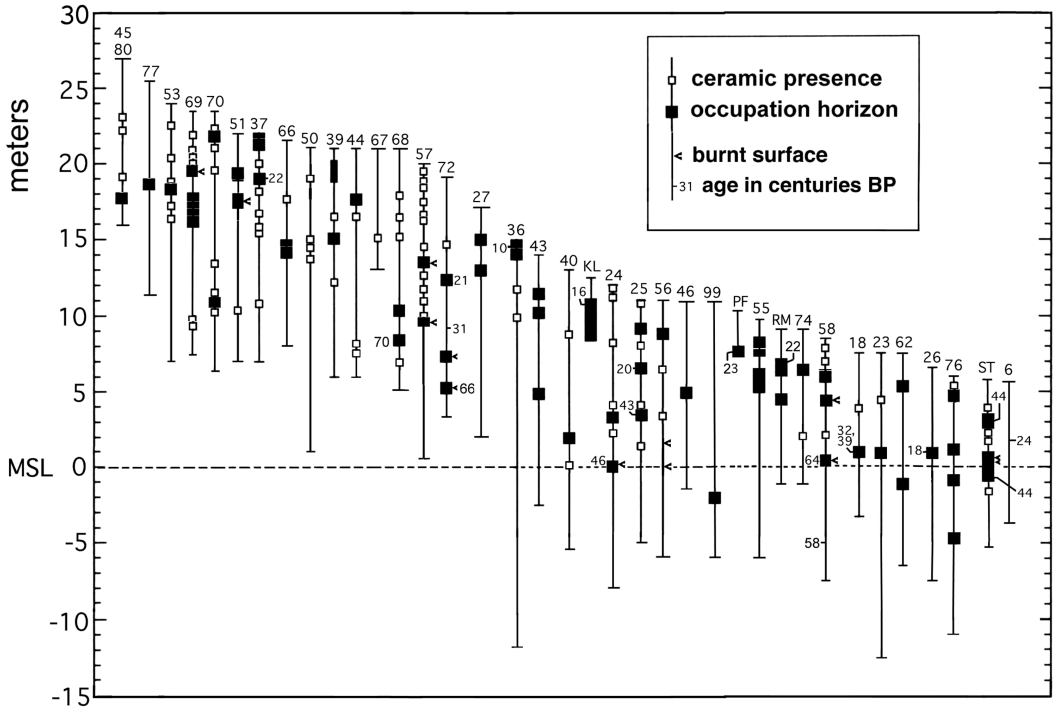

Figure 4. Vertical profiles of boreholes and excavated sites, arranged in rank order of local surface elevation above mean sea level. The horizontal axis has no scale, because the boreholes and sites are dispersed over a broad area. The surface is at the top of each column, which is labeled by borehole number or site area (letters). Underlined labels in Figure 3 indicate locations of most of these boreholes and sites. Dated samples are labeled alongside some profiles in hundreds of years before present. Some ceramic fragments and stones showed burnt surfaces.

were not continuously cased during drilling, some dated samples may have fallen from shallower horizons, resulting in anomalously young ages for a given depth.

The occupation horizons dated by diagnostic ceramics from the excavations are generally shallower than the borehole samples of comparable apparent age that were dated by radiocarbon and ceramic luminescence. Figure 5 shows this discrepancy, which may be due in part to a selection effect, since the excavations were limited to a depth of about 4 m, and some of the archaeological horizons may extend well below that. However, the systematic appearance of the offset suggests that other causes, not yet understood, may also be at work. In general, age–depth correlations based on the archaeological excavation of diagnostic ceramics will be far more reliable than those based on dating samples from boreholes, although the latter data greatly extend the range of accessible depths.

Despite the range of borehole surface elevations, the varied deposition regimes in the delta, and the anomalous outlying data points, the scatter for most of the dated samples in Figure 5 defines a broad age–depth trend. The slope of this trend suggests an average sediment deposition rate of about 2.5 m/kyr for the last 8 kyr and a rate perhaps ten times higher than that in earlier times. The dramatic change in the

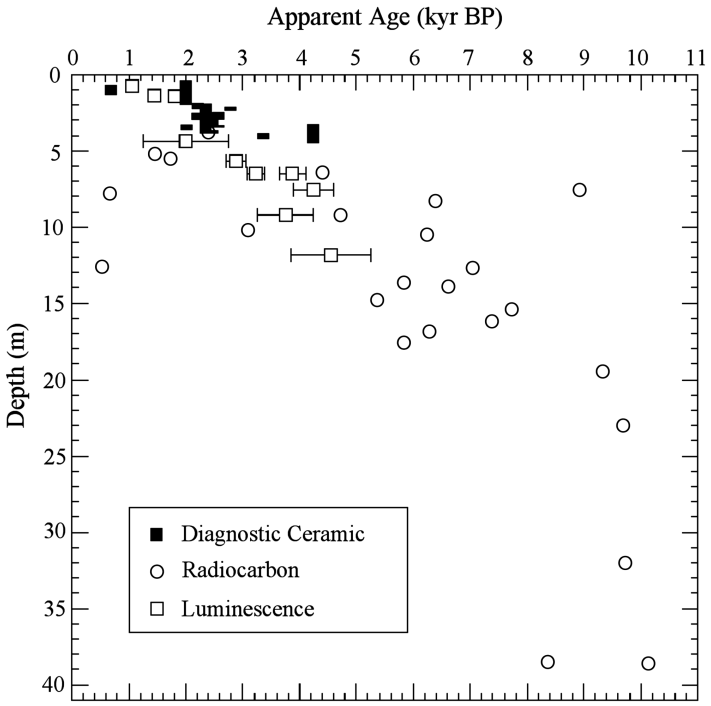

Figure 5. Plot of apparent age of dated samples in thousands of years before present (1950 A.D.), versus depth below the surface in meters (data from Tables I and II and Soter & Katsonopoulou, 1998). Solid rectangles, open squares, and open circles represent, respectively, archaeologically diagnostic ceramics, nondiagnostic ceramic fragments dated by optical luminescence, and organic matter dated by radiocarbon.

deposition rate probably reflects the global deceleration in the rise of sea level around 8 kyr B.P., caused by the final melting of the Laurentide ice sheet. Marine deltas throughout the world show a similar change in deposition rate at about the same time (Stanley & Warne, 1994). For the last thousand years, the age–depth trend suggests a very slow rate of net deposition, perhaps due to increased erosion associated with tectonic uplift of the delta.

We encountered both the Classical and EBA horizons at about 3 to 4 m below the present surface, although they differ in age by some 2000 years. Borehole B75, located within the EBA site, provides a possible explanation. It contained a dense sequence of occupation horizons extending from about 3.0 to 6.6 m depth (Alvarez-Zarikian, Soter, & Katsonopoulou, 2008:Figure 6). A charcoal fragment from the base of this sequence gave a radiocarbon date of 4400 B.P. (still in the EBA), so the entire sequence may have been deposited in only a few hundred years. This suggests the possibility that the EBA settlement is on an artificial mound, or *tell*, which rose about 3 m above the surrounding landscape of that period. Excavation of trench H61 established that the EBA horizon continues at least down to 4.5 m in this area, and a test core in the trench showed that layers containing pottery and stones continue down to 5.8 m.

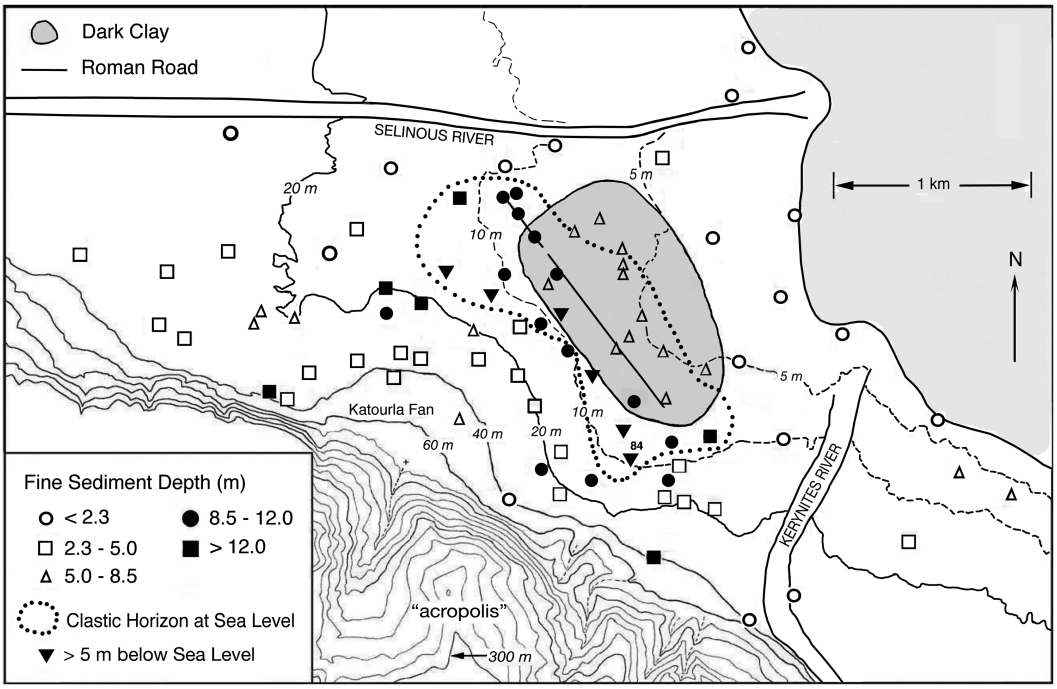

Figure 6. Chart of boreholes indicates the depth of horizon C (the top of the first coarse clastic layer below the surface). The dotted contour encloses the area where horizon C is below current sea level (based on nominal elevation data, ca. 1966). Solid triangles mark boreholes where this transition between fine and coarse material is both more than 12 m below the surface and more than 5 m below sea level. The solid contour encloses the area (shaded) of a distinctive black clay layer, probably deposited in a freshwater marsh.

STRATIGRAPHY AND PALEOENVIRONMENTS

The stratigraphy of the coastal plain is extremely heterogeneous, due to highly variable deposition and erosion on this geologically active fan delta (Soter et al., 2000). Floods and shifting distributaries from the rivers produced a patchwork of fine and coarse deposits over much of the delta, until the Selinous and Kerynites Rivers were confined by levees starting in the 1930s. The resulting stratigraphy can vary greatly over horizontal scales of only a few meters, as found in boreholes and trenches.

The upper strata usually consist of fine sediments (clay, silt, or sand). Next comes a deposit of clastic material, with gravel, pebbles, or cobbles, usually more than a meter thick. We refer to the top of this clastic layer as horizon C. The thickness of fine sediments deposited above horizon C varies across the Helike Delta, as shown in Figure 6. Horizon C is generally less than 5 m deep on the Katourla Fan, dips steeply around the periphery of the fan, and then gradually rises toward the sea. The solid triangles in Figure 6 define an elongated arc-shaped zone where horizon C is deepest. This trough or axis of the depression in horizon C is at least 5 m below nominal sea level (ca. 1966).

Horizon C lies below sea level for most boreholes with surface elevations between 5 and 10 m. Borehole B84 (labeled) reached 22 m depth below a surface elevation of

9 m, but did not penetrate horizon C. The dotted contour in Figure 6 encloses the area where horizon C lies below nominal sea level, which suggests the location of an ancient lagoon, bounded by a barrier beach.

Horizon C dips more steeply toward the axis of the depression on the landward (southeast) side than on the seaward (northwest) side. The pebbles in the landward side are generally angular, while those in the seaward side are more rounded. The former may consist of terrestrial flood deposits from the Katourla Fan, while the latter may represent marine beach deposits which prograded and aggraded with rising sea level. Another possibility is that the dip of horizon C on the seaward side of the axis reflects back-tilting of the hanging wall block of the Helike Fault. A third interpretation is that the trough in horizon C marks the depression formed at the head of the landslide triggered by the Classical earthquake, according to the hypothesis of Ferentinos and Papatheodorou (2005).

We analyzed many borehole and trench samples for evidence of the ancient depositional environments. The most useful indicators were shells of ostracods and foraminifera, which are microfauna with preferred habitat ranges influenced by salinity. Figure 7 shows the schematic profiles of boreholes and trenches from which we analyzed environmental indicators in sediment samples (Soter et al., 2001; Alvarez-Zarikian, Soter, & Katsonopoulou, 2008). The numbers alongside some profiles give the ages of dated samples in hundreds of years B.P. Samples from the upper parts of the profiles indicate mainly freshwater and brackish depositional environments, while most samples found deeper than about 5 m below nominal sea level represent marine environments. The upward transition in the cores from marine to either brackish or freshwater deposition dates from about 7 kyr B.P., which corresponds approximately to the change in slope of the age–depth trend shown in Figure 5.

Some individual samples contain a mixture of indicators of different environments. These may represent transitional environments (for example, lagoons with seasonal variation in salinity) or a mixture of sediments transported from different environments. Some samples, marked by an asterisk (*) in Figure 7, contain broken or abraded microfossils, probably due to wave action in a high-energy environment (data in Soter et al., 2000; Alvarez-Zarikian, Soter, & Katsonopoulou, 2008). Several boreholes and trenches yielded sediments containing microfossils that were both abraded and derived from different environments. We found such assemblages in borehole B14 at 11.6 m depth, in B16 at 7.7 m, in B58 at 2.65 and 12 m, and in trenches H1 at 3.85 m, H7 at 2.6 to 3.1 m, and H19 at 1.45 and 2.6 to 3.2 m. Some of these samples may reflect the influence of tsunami deposition.

In the Figure 3 map, asterisks mark the locations of boreholes and trenches that yielded such assemblages. For example, in the Romanos site (RM), just below the Hellenistic wall at 3.85 m in trench H1, we found a deposit of fine stratified sand containing abraded brackish and marine ostracods and foraminifera, perhaps deposited by the tsunami of 373 B.C. However, the Romanos site may have been only a few hundred meters from the ancient shoreline, so we cannot exclude the possibility of a storm surge deposit. In addition, sand blows caused by earthquakes can erupt and deposit sheets of sand arising from ancient marine strata buried well below the surface.

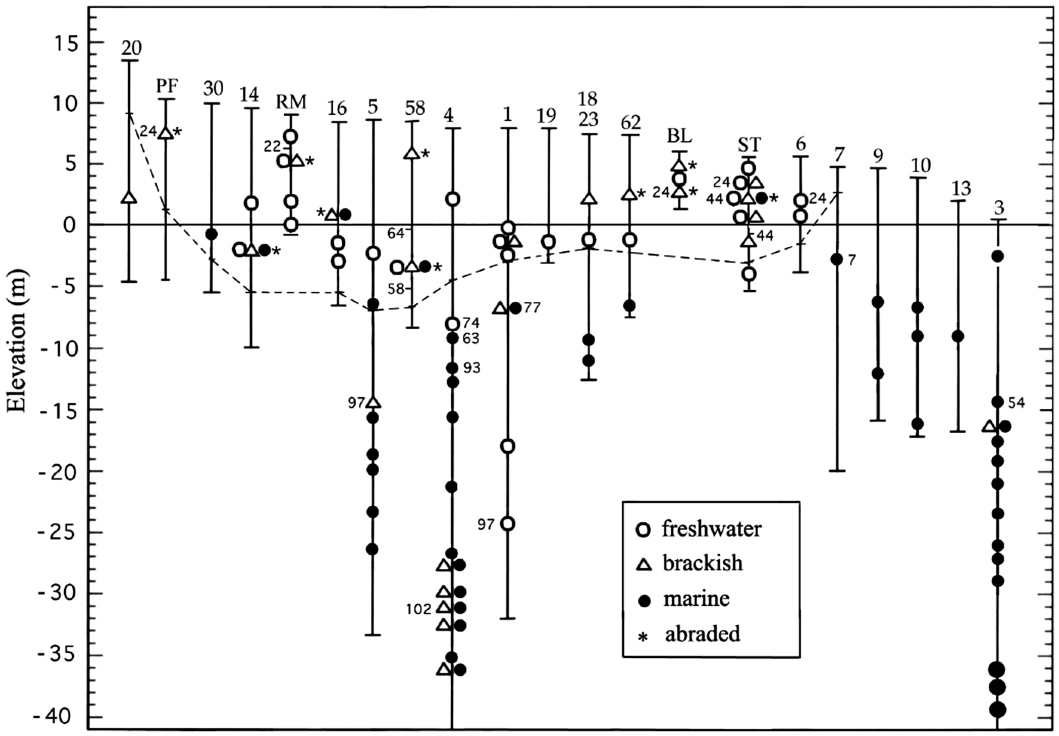

Figure 7. Vertical profiles, in rank order of nominal surface elevation, showing borehole and trench samples analyzed for environment of deposition based on microfossils (data in Soter et al., 2001, and Alvarez-Zarikian, Soter, & Katsonopoulou, 2008). Each profile is labeled at the top by its borehole number or site code. Dated samples are labeled alongside some profiles in hundreds of years before present. Samples analyzed for environment are indicated by symbols for "freshwater" (lakes, ponds, marshes), "brackish" (lagoonal or nearshore), and "marine" (prodelta) facies. Samples labeled with more than one symbol represent transitional environments or mixed sediments redeposited from different environments. Asterisks (*) denote abraded or fragmented microfossils, indicating severe reworking due to wave action. Where this occurs in an assemblage of microfossils from a mixture of environments, such damage may reflect the influence of a tsunami. The dashed line represents horizon C, the contact between the upper fine sediments and the first coarse clastic horizon below.

Dawson and Stewart (2007) emphasize that it is generally difficult in wave-dominated shallow marine settings to distinguish tsunami deposits from background storm deposits, both because they resemble each other and because subsequent storms can modify or remove the traces of tsunamis. This is especially true in a case like ours, where the evidence is confined to trenches and boreholes in a high-energy deltaic environment subjected to erosive flooding. The criterion we used to suggest evidence of a tsunami is the presence of abraded microfauna with a mixture of marine, brackish, and freshwater taxa. In view of the problems noted above, however, our interpretation remains hypothetical.

The dashed line in Figure 7 represents horizon C, the contact between the upper fine sedimentary strata and the first major coarse clastic layer below. The prevalence of fresh and brackish water indicators in the fine sediments above horizon C suggests that those strata were deposited in a lacustrine–lagoonal environment.

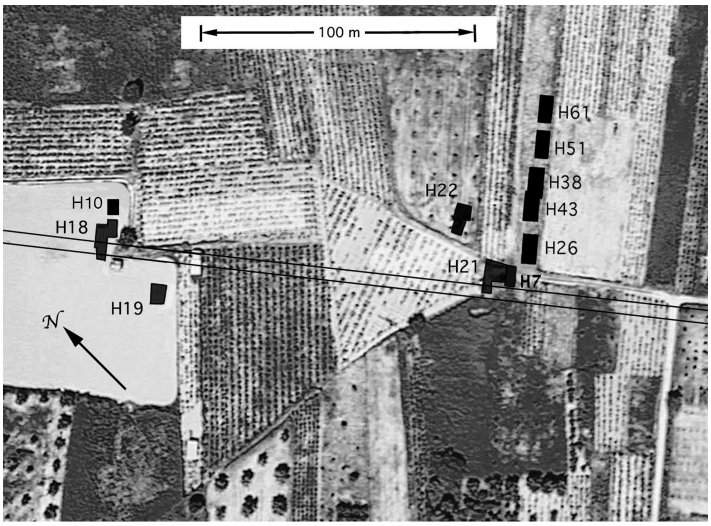

Figure 8. Infrared aerial photograph shows the Classical and Early Bronze Age sites. Black areas show the locations of three trenches in the Classical area (Balalas) and eight trenches in the Early Bronze Age area (Saitis). Trenches H7 and H21 are contiguous, as are H38 and H43. The double line traces the Roman road, which intersects H18 and H21.

In boreholes and trenches in the central part of the delta, we found a shallow layer of black clay, about 0.7 km^2 in area, shown by the shaded region in Figure 6. This layer is usually 20 to 40 cm thick and its upper surface is 1 to 2 m below ground in the western half of the area, increasing to about 3 m in the eastern half. The black clay was deposited in an undisturbed organic-rich anoxic environment—probably a marsh. Sediment samples of this layer (from H7 in the EBA area and H10 and H19 in the Classical area) contained freshwater microfossils only. The surface of the Roman road lies just below the black clay layer in H18 and H21, which suggests that a shallow marsh covered this portion of the road in Byzantine times.

The Late Byzantine, Roman, and Hellenistic sites are at higher elevations than the Classical and EBA sites and are covered only by terrestrial floodplain deposits. They are located for the most part outside the area of the black clay layer and were evidently never submerged by long-standing bodies of water.

OBSERVATIONS IN THE CLASSICAL AND EARLY BRONZE AGE AREAS

The aerial infrared photograph in Figure 8 shows three trenches excavated in the Classical area (BL site, left) and eight trenches in the Early Bronze Age area (ST site, right), together with the Roman road, which intersects trenches H18 and H21.

Trench H19 revealed the corner of a Classical building 3 m below the surface (Figure 9). Only the corner of the building remains *in situ*; everything else was apparently swept away. A destruction layer of stones from one wall appears to have been thrown down exactly in the seaward direction. All the pottery from trench H19 consisted of small worn fragments, many of them found inside the corner. The pattern of destruction is consistent with the damage expected from a tsunami, where

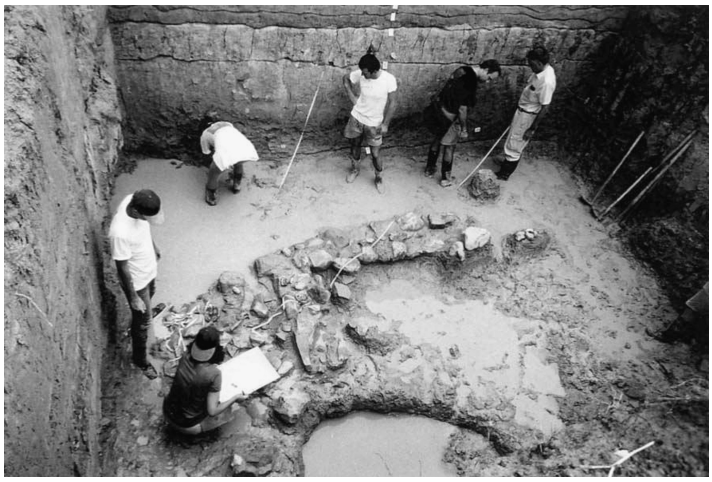

Figure 9. Trench H19, showing the corner foundation of a Classical building about 3 m below the surface. This occupation horizon is below the water table. The upper courses of one wall have fallen outside the building in the direction toward the sea (to the left).

the backwash flow is generally more erosive than the run-up (Dawson & Stewart, 2007).

Figure 10 shows seven trenches excavated in the Early Bronze Age area. The Roman road crosses the west side of H21 at a depth of about 1.8 m, while EBA walls lie about 3.3 m below the surface on the other side. All seven trenches revealed well-preserved EBA walls, numerous intact pottery vessels, and evidence of conflagration-blackened pottery, charcoal, and sediment darkened by ash.

Trenches H22 and H43 contain cobbled EBA streets flanked by rectangular buildings. H22 also has an apsidal building. A long wall in H22 is broken by a right lateral offset of about 25 cm (Figure 11), possibly due to motion on a strike slip fault oriented NW-SE. If an earthquake caused this offset, we do not know whether it occurred in connection with the drowning of the site or much later. This wall belongs to the final phase (EH III) of the settlement. We found no other evidence for an earthquake or strike-slip motion in the ST site.

Figure 12 shows the stratigraphic profiles of trenches H18 and H19 in the Classical area and trenches H7 + H21 (combined data from contiguous trenches) and H22 in the Early Bronze Age area. Blocky symbols alongside the columns indicate the upper levels of ancient walls. In H18 and H22, walls shown at different depths are in different parts of the trench. Open circles, triangles, and closed circles indicate, respectively, freshwater, brackish, and marine depositional environments, based on the analysis of microfossils in sediment samples from H19 and H7 by Alvarez-Zarikian, Soter, and Katsonopoulou (2008). The stratigraphic sequence in H7 from top to bottom is: L1 surface soil, L2 reddish brown silt, L3 yellowish sandy silt, L4 reddish clay, L5 dark brown clay, L6 fine sand and gravel, L7 black clay, L8 gray and brown clay, L9 gray and olive clay, L10 dark gray clay containing the EBA occupation horizon.

Trenches H18 and H19 in the Classical site are about 30 m apart and share the same general stratigraphy throughout. Trenches in the Classical and EBA areas also share the same stratigraphy but only for the deeper layers, from L6 or L7 and

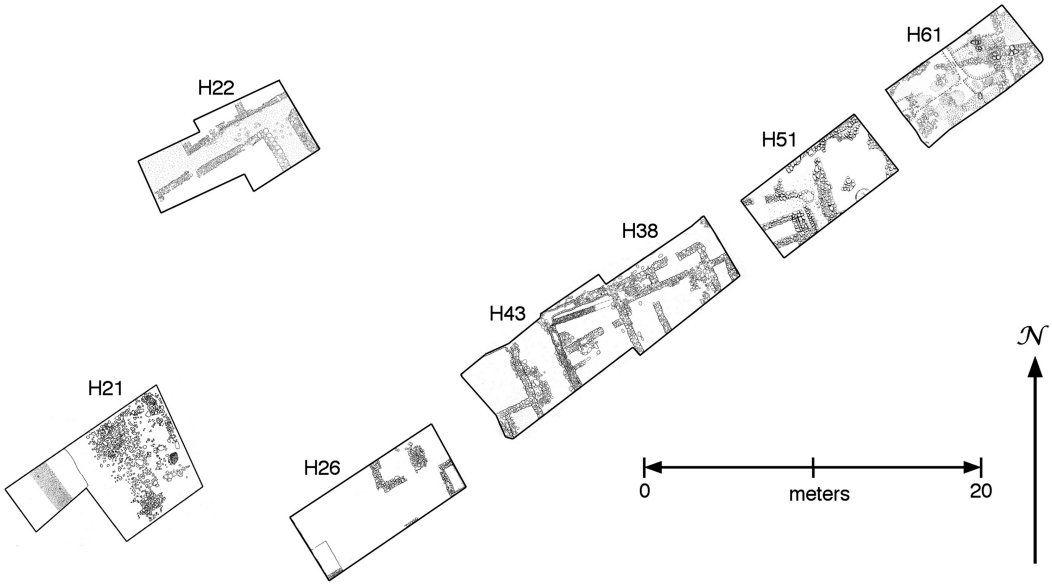

Figure 10. Plan of trenches excavated in the Early Bronze Age area. The wall foundations are 3.3 to 4.5 m below ground.

Figure 11. Trench H22, looking northeast. Note the right lateral strike-slip through the long wall.

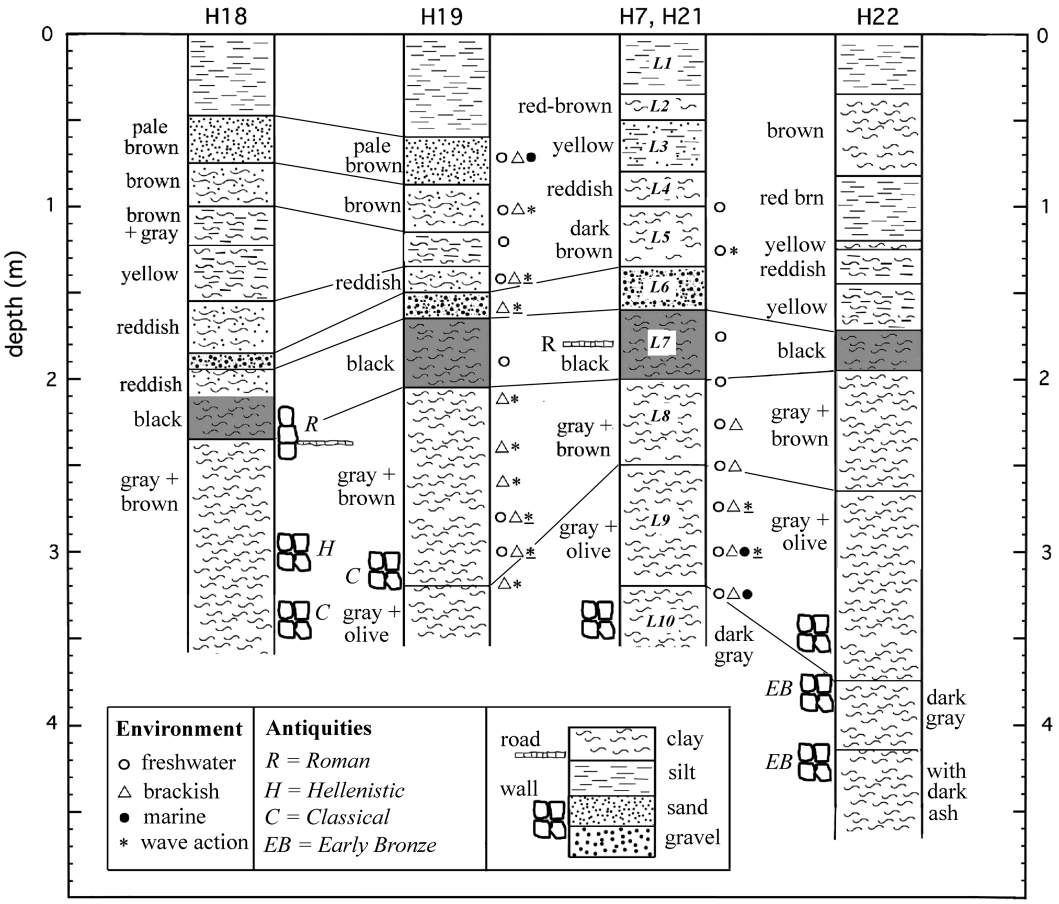

Figure 12. Stratigraphic profiles of trenches H18 and H19 in the Classical area and trenches H7, H21, and H22 in the Early Bronze Age area. The two areas are about 130 m apart. Data from the contiguous trenches H7 and H21 are combined in a single profile. The strata in H7/H21 are numbered. The black clay layer L7 occurs in all sections. Symbols alongside the columns represent depositional environments and the presence of architectural elements. Underlined asterisks indicate possible microfaunal evidence for tsunami deposition. Some depths represent average values, because some strata are inclined and walls of a given period may occur at different levels in different parts of the same trench. (The profile for H21 is for the northeast side of the trench. The Roman road crosses the opposite or western side, where the inclined layer L7 is deeper. The road thus lies below that layer, despite the appearance in the figure.)

downward. The extensive freshwater black clay layer L7 may date from the Byzantine period, because it overlies the Roman road in H18 and H21.

The gray and brown clay layer L8 apparently dates from the Classical period. In trenches H18 and H19, we found Classical pottery together with walls in the lower part of this layer. In trenches H19 and H7, layer L8 contains brackish and freshwater microfossils, with the brackish ones abraded in H19. This layer was evidently deposited in a lagoon. Trench H8, about 50 m southwest of H21, not shown here, had the same sequence of strata as H21, but no ancient structures. Layer L8 in that trench yielded many ceramic fragments dating from the Classical and Archaic periods.

The gray and olive clay layer L9 appears to date from Archaic to Classical times. The dark gray clay layer L10 dates from the EBA. In trenches H7 + H21 and H22, we found buildings with EBA pottery at the top of layer L10. Trenches H18 and H19 in the Classical area were not deep enough to encounter the EBA layer L10, if it exists in that location. Layer L9 in H7 contains freshwater and abraded brackish and marine microfossils.

Layer L8 in trench H19 and layer L9 in trench H7 both contain abraded brackish water microfossils. This damage may be due to centuries of wave action from storms washing across the shallow lagoons that apparently covered both drowned sites. Some of the abrasion in layer L8 of trench H19 may also be due to the historical tsunami. However, the expected sandy deposit was not observed; subsequent mixing may have dispersed it in the prevailing clay. While the historical evidence for the earthquake and tsunami in 373 B.C. is strong, evidence based on stratigraphy and archaeological excavation is merely suggestive. Detailed analysis of additional samples would be needed to establish it.

CHANGES OF LOCAL SEA LEVEL

The once-submerged Classical and Early Bronze Age horizons both lie well above the present sea level. The latter would be ca. 6 m below the surface at both sites, based on nominal elevation measurements (dating from 1966), according to the military map. Even using contemporary elevation data for selected survey points, sea level would be 4.5 and 3.7 m below the surface at the Classical and EBA sites, respectively, which is still below some of the drowned occupation horizons. Soter (1998) suggested that tectonic forces have uplifted the Helike Delta by several meters since antiquity. This could account for the elevation above sea level of the brackish and marine indicators in layers L8 and L9.

Evidence from older sediments in boreholes supports the case for net uplift of the delta. The curve in Figure 13 models the rise of sea level in the region as a function of time during the Holocene, relative to present sea level at 0 m. It was derived from the global eustatic sea level data of Fleming et al. (1998), corrected for the regional isostatic compensation appropriate to the Gulf of Corinth using the model of Lambeck (1995) and Lambeck and Purcell (2005). See also Soter (1998).

The points in Figure 13 represent dated sediment samples containing brackish and/or marine microfossils, from three deep boreholes (B1, B4, B5) and from the EBA and Classical sites (ST and BL, respectively). The points are plotted versus present nominal depth. The brackish samples were presumably deposited at or below the elevation given by the sea level curve at the times corresponding to their ages, and the marine samples were deposited below the sea level curve. Most of the points fall well above the sea level curve, which suggests that uplift of the Helike Delta has more than compensated for co-seismic subsidence events during the Holocene.

Figure 14 is a simplified hypothetical model for the recent evolution of the Helike Delta. In this schematic profile, the vertical dimension is highly exaggerated. The line HF represents the Helike Fault (the actual fault dip is about 55°). The average

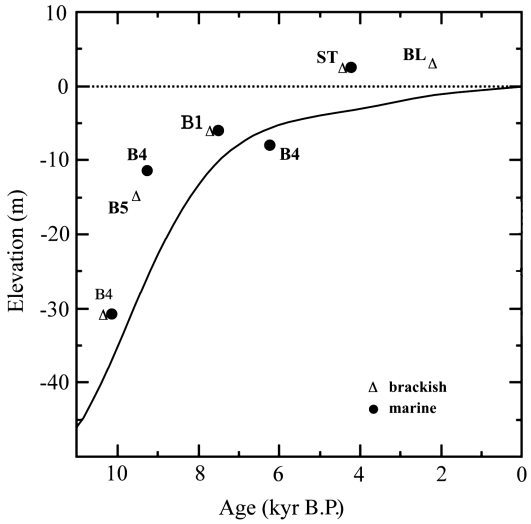

Figure 13. Model curve of eustatic plus regional isostatic sea level during the last 10 kyr relative to present elevation, for the Gulf of Corinth, from data of Fleming et al. (1998), Lambeck (1995), and Lambeck and Purcell (2005). Points represent dated sediment samples containing brackish and/or marine microfossils from boreholes B1, B4, and B5 (Figure 7) and from the Early Bronze Age (ST) and Classical (BL) sites. Brackish samples were presumably deposited at or near sea level. Tectonic uplift of the delta may account for the elevation of these horizons above the sea level corresponding to the time of their deposition.

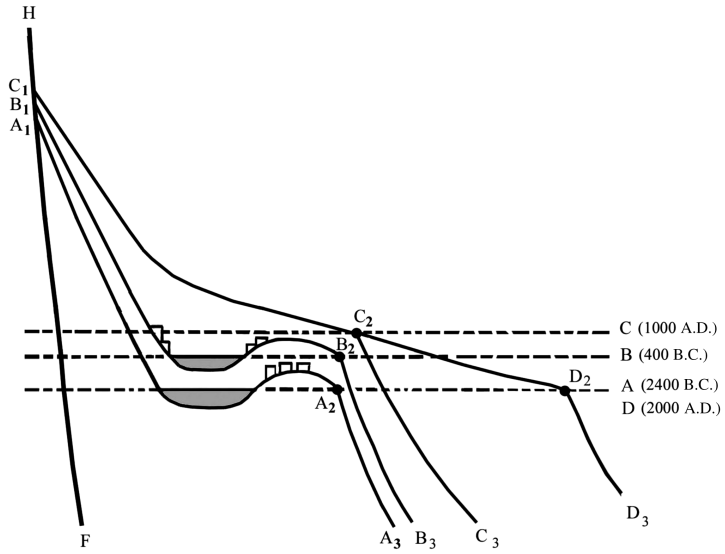

Figure 14. Schematic model suggests a hypothetical evolution of the Helike Delta. The vertical dimension is highly exaggerated. HF is the Helike Fault. Shaded basins represent lagoons and rectangles indicate settlements. Horizontal dashed lines indicate local sea levels relative to the delta block. Profiles A, B, C, and D represent the delta surface corresponding to times 2400 B.C., 400 B.C., A.D. 1000, and A.D. 2000, respectively, and the black dots represent the corresponding shorelines. Seismic subsidence events caused a relative rise of local sea level from A to B and from B to C, while tectonic uplift of the delta caused relative lowering of sea level from C to D.

distance from the fault trace to the present shoreline at D_2 in this region is about 2 km. The horizontal dashed lines represent local sea level relative to the basement of the delta block at the labeled times. The solid line profiles A, B, C, and D correspond to the delta surface at approximately 2400 B.C., 400 B.C., A.D. 1000, and A.D. 2000, respectively. Solid dots represent the corresponding shoreline locations. The shaded basins and small rectangles represent lagoons and settlements, respectively.

The profile $A_1A_2A_3$ represents the surface prior to submergence of the Early Bronze Age site, which is shown on the seaward shore of a lagoon. Rapid subsidence of the delta, perhaps triggered by an earthquake, raised the local sea level to the dashed line B, drowning the EBA settlement. Sedimentation then gradually raised the surface to $B_1B_2B_3$, and some settlements of Classical Helike were built around the shores of a smaller lagoon. The earthquake of 373 B.C. caused rapid submergence of the delta, raising the local sea level to the dashed line labeled C and drowning the Classical city. Continued sedimentation raised the surface to the profile $C_1C_2C_3$. Tectonic uplift of the delta subsequent to the Classical earthquake has returned relative sea level to nearly the elevation it had ca. 2400 B.C., and sedimentation extended the delta surface by progradation to D_2. According to this model, tectonic uplift and erosion reduced the sediment accumulation on the upper delta surface C_1C_2 during the last millennium, in agreement with the age–depth trend derived from the borehole data (Figure 5). The recent progradation would also account for the absence of antiquities in boreholes and trenches in the nearshore area C_2D_2. While the model is consistent with all our observations, we emphasize that it remains entirely hypothetical.

CONCLUSIONS

The results from archaeological excavations and boreholes reveal dramatic changes in the environment of the Helike Delta during the last 10,000 years. A thick layer of fine-grained sediments deposited in fresh and brackish water dominates the central part of the delta (most prominent within the dotted contour in Figure 6). A coarse clastic deposit at the base of this unit generally dips landward, perhaps due to progradation and aggradation of the ancient shoreline with rising sea level. The inclination may also reflect back-tilting of the delta block, which lies on the hanging wall of the Helike Fault. The resulting basin evidently supported an intermittent lagoon, which extended to the foot of the Katourla Fan from the Late Neolithic to the Late Roman period. The Early Bronze Age settlement was built in this area, perhaps on a modest topographic rise or tell (about 3 m high) on the seaward side of the lagoon. The adjacent Classical site would also have been situated near or around a lagoon.

Our interpretation of the observations suggests that two major episodes of subsidence, separated by about 2000 years, caused drowning and abandonment of settlements on the Helike Delta. The first, in the Early Bronze Age (ca. 2200/2150 B.C.), submerged a major coastal settlement in a lagoon, which later silted over. The EBA buildings are unusually well preserved, with much of the pottery intact, buried under

3 to 5 m of fine-grained sediments containing marine, brackish, and freshwater microfauna. While an earthquake may have triggered the subsidence of the EBA settlement, we found no evidence of associated damage by a tsunami.

Subsequent sedimentation and uplift raised the level of the delta surface to keep pace with a few meters rise in isostatic sea level. This allowed reoccupation of the area, which included the development of Archaic and Classical Helike. The city lasted until a catastrophic earthquake triggered the abrupt subsidence and drowning of the site in a lagoon. Unlike the submergence of the EBA settlement, the historic event of 373 B.C. was accompanied by a powerful tsunami, which may have swept away the foundations of many exposed buildings.

After that catastrophe, a Hellenistic settlement was built on the northern margin of the lagoon, extending up to the adjacent foothills. Following the construction of a major Roman road near the sea in the Augustan period, a Roman settlement arose on the southeastern margin of the lagoon, extending along the southern part of the plain near the foothills. An earthquake in the 5th century A.D. destroyed the Roman site. In Byzantine times, a marsh covered the area of the excavated Classical and EBA sites, as indicated by a shallow black clay stratum with freshwater microfossils, and a Late Byzantine settlement occupied the area northwest of the marsh.

Tectonic changes of relative sea level have also affected other ancient coastal settlement in the northern Peloponnesos. In the region east of Helike, geoarchaeology provides additional evidence for episodes of coastal uplift and/or subsidence. The Roman harbor of Aigeira (Figure 2 inset) was uplifted by about 4 m within the last 2000 years, and the initial phase of uplift must have been sudden (Papageorgiou et al., 1993; Stiros, 1998). At Lechaion, the western harbor of ancient Corinth, borings by marine mollusks in the masonry walls of a harbor channel are now about a meter above sea level (Stiros et al., 1996). However, the foundations of an ancient building are partly submerged on the beach. The evidence therefore suggests "complex up and down vertical displacement, with uplift clearly predominant . . ." (Stiros & Pirazzoli, 1998). At Kenchreai, the eastern harbor, about 9 km southeast of Corinth on the Saronic Gulf, an ancient mole with extensive foundations of buildings is now submerged as much as 4 m. Archaeological evidence suggests that three earthquakes between the 1st and 6th centuries A.D. submerged the site, with subsidence events each of order 0.8 m (Scranton, Shaw, & Ibrahim, 1978).

At Cape Trelli, near Korphos, 30 km southeast of Corinth on the Saronic Gulf, Tartaron, Rothaus, and Pullen (2003) reported three layers of beachrock submerged at 1.2, 3.3, and 5.9 m below sea level. Each is full of ceramic fragments cemented in place; those in the lowest layer are of Mycenaean age. Since beachrock is formed rapidly in the intertidal zone near sea level, this evidence suggests the occurrence of several episodes of subsidence since the Late Bronze Age. Large quantities of Mycenaean pottery on the adjacent beach and an extensive complex of "cyclopean" walls on the adjoining land suggest the presence of an important Bronze Age harbor that would have been seriously affected by seismic subsidence.

We gratefully acknowledge the Tria Epsilon Group of Companies in Athens and the Institute for Aegean Prehistory in Philadelphia for contributions to the Helike Project. We also wish to thank John C. Kraft, Helmut Brückner, Elias Sotiropoulos, and Jean-Daniel Stanley, who generously provided expert guidance over many years. Finally, we thank two reviewers and an associate editor for their careful reading of the manuscript and their valuable critical comments.

REFERENCES

Alvarez-Zarikian, C., Soter, S., & Katsonopoulou, D. (2008). Recurrent submergence and uplift in the area of ancient Helike, Gulf of Corinth, Greece: Microfaunal and archaeological evidence. Journal of Coastal Research, 24, 110–125.

Anderson, J.K. (1954). A topographical and historical study of Achaea. Annual of the British School at Athens, 49, 72–92.

Dawson, A.G., & Stewart, I. (2007). Tsunami deposits in the geological record. Sedimentary Geology, 200, 166–183.

Ferentinos, G., & Papatheodorou, G. (2005). The disappearance of ancient Helike: New geological evidence (in Greek). In D. Katsonopoulou, S. Soter, & I.K. Koukouvelas (Eds.), Ancient Helike and Aigialeia: Archaeological sites in geologically active regions, Third International Conference (pp. 203–220). (English abstract online at www.cprm.gov.br/33IGC/1352910.html.)

Fleming, K., Johnston, P., Zwartz, D., Yokayama, Y., Lambeck, K., & Chappell, J. (1998). Refining the eustatic sea-level curve since the Last Glacial Maximum using far- and intermediate-field sites. Earth and Planetary Science Letters, 163, 327–342.

Katsarou-Tzeveleki, S. (in press). Morphology and distribution of pottery at the Early Helladic settlement of Helike. In D. Katsonopoulou (Ed.), Ancient Helike and Aigialeia: The early Helladic Peloponnesos, Fourth International Conference, Helike IV.

Katsonopoulou, D. (1995). Helike (in Greek). Archaiologia, 54, 40–45.

Katsonopoulou, D. (1998). The first excavation at Helike: Klonis field (in Greek). In D. Katsonopoulou, S. Soter, & D. Schilardi (Eds.), Ancient Helike and Aigialeia, Second International Conference (pp. 125–146).

Katsonopoulou, D. (2002). Helike and her territory in the light of new discoveries. In E. Greco (Ed.), Gli achei e l'identita etnica degli achei d'occidente. Fondazione Paestum. Tekmeria, 3, 205–216.

Katsonopoulou, D. (2005a). The earthquake of 373 BC: Literary and archaeological evidence. In D. Katsonopoulou, S. Soter, & I.K. Koukouvelas (Eds.), Ancient Helike and Aigialeia: Archaeological sites in geologically active regions, Third International Conference (pp. 15–32).

Katsonopoulou, D. (2005b). Test excavations in the Helike Delta in 2000 and 2001: Preliminary results. In D. Katsonopoulou, S. Soter, & I.K. Koukouvelas (Eds.), Ancient Helike and Aigialeia: Archaeological sites in geologically active regions, Third International Conference (pp. 33–65).

Katsonopoulou, D. (2007). An early Helladic settlement at Helike (in Greek). In E. Konsolaki-Giannopoulou (Ed.), ΕΠΑΘΛΟΝ, International archaeological conference presented to Adonis K. Kyrou (pp. 117–126). Athens: Municipality of Poros.

Katsonopoulou, D. (2010). The Hellenistic dye-works at Helike, Achaea, Greece. In C. Alfaro, J.P. Brun, P. Borgard, & R. Pierobon Benoit (Eds.), Purpureae vestes III: Textiles and dyes in antiquity (pp. 217–222). Naples: University of Valencia and Centre Jean Berard .

Katsonopoulou, D. (2011a). Pausanias' travel from Helike of Achaea to Aristonautes in Korinthia. In Korinthia and northeastern Peloponnesos: Topography and history from the prehistoric times to late antiquity. Proceedings of International Conference, German Institute at Athens and LZ Ephorate of Antiquities at Corinth (in press).

Katsonopoulou, D. (2011b). The Early Helladic settlement at Helike: An Early Bronze Age center in Achaea. In D. Katsonopoulou (Ed.), Ancient Helike and Aigialeia: The Early Helladic Peloponnesos, Fourth International Conference, Helike IV (in press).

Koukouvelas, I.K., Katsonopoulou, D., Soter, S., & Xypolias. P. (2005). Slip rates on the Helike Fault, Gulf of Corinth, Greece: New evidence from geoarchaeology. Terra Nova, 17, 158–164.

Koukouvelas, I.K., Stamatopoulos, L., Katsonopoulou, D., & Pavlides, S. (2001). A paleoseismological and geoarchaeological investigation of the Eliki fault, Gulf of Corinth, Greece. Journal of Structural Geolology, 23, 531–543.

Kutrubes, D.L., Soter, S., Katsonopoulou, D., & Heinze, A. (2003). Ground penetrating radar in the search for ancient Helike, Greece. SAGEEP Proceedings (pp. 92–106).

Lambeck, K. (1995). Late Pleistocene and Holocene sea-level change in Greece and south-western Turkey: A separation of eustatic, isostatic and tectonic contributions. Geophysical Journal International, 122, 1022–1044.

Lambeck, K., & Purcell, A. (2005). Sea-level change in the Mediterranean Sea since the LGM: Model predictions for tectonically stable areas. Quaternary Science Reviews, 24, 1969–1988.

Leonards, G.A., Sotiropoulos, E.S., & Kavvadas, M.J. (1988). Helice: The lost town of ancient Greece. In P.G. Marinos & G.C. Koukis (Eds.), Engineering geology of ancient works, monuments and historical sites (pp. 1307–1313). Rotterdam: Balkema.

Marinatos, S. (1960). Helice: A submerged town of Classical Greece. Archaeology, 13, 186–193.

Mouyaris, N., Papastamatiou, D., & Vita-Finzi, C. (1992). The Helice fault? Terra Nova, 4, 124–129.

Papadopoulos, G. (1998). A reconstruction of the great earthquake of 373 BC in the western Gulf of Corinth. In D. Katsonopoulou, S. Soter, & D. Schilardi (Eds.), Ancient Helike and Aigialeia, Second International Conference (pp. 479–494).

Papadopoulos, G.A., Vassilopoulou, A., & Plessa, A. (2000). A new catalogue of historical earthquakes in the Corinth Rift, central Greece: 480 BC–AD 1910. In G.A. Papadopoulos (Ed.), Historical earthquakes and tsunamis in the Corinth Rift, central Greece (pp. 9–110). Athens: Institute of Geodynamics, National Observatory of Athens.

Papageorgiou, S., Arnold, M., Laborel, J., & Stiros, S.C. (1993). Seismic uplift of the harbour of ancient Aigeira, central Greece. International Journal of Nautical Archaeology, 22, 275–281.

Pavlides, S.B., Koukouvelas, I.K., Kokkalas, S., Stamatopoulos, l., Keramydas, D., & Tsodoulos, I. (2004). Late Holocene evolution of the East Eliki fault, Gulf of Corinth (Central Greece). Quaternary International, 115–116, 139–154.

Pirazzoli, P.A., Stiros, S.C., Fontugne, M., & Arnold, M. (2004). Holocene and Quaternary uplift in the central part of the southern coast of the Corinth Gulf (Greece). Marine Geology, 212, 35–44.

Schmidt, J.F.J. (1875). Studien über Erdbeben. Leipzig: Scholtze.

Scranton, R., Shaw, J.W., & Ibrahim, L. (1978). Kenchreai, eastern port of Corinth, Vol. 1. Leiden: Brill.

Soter, S. (1998). Holocene uplift and subsidence of the Helike Delta, Gulf of Corinth, Greece. In I. Stewart & C. Vita-Finzi (Eds.), Coastal tectonics (pp. 41–56). Special Publication 146. London: Geological Society.

Soter, S., & Katsonopoulou, D. (1998). The search for ancient Helike, 1988–1995: Geological, sonar and borehole studies. In D. Katsonopoulou, S. Soter, & D. Schilardi (Eds.), Ancient Helike and Aigialeia, Second International Conference (pp. 67–116).

Soter, S., & Katsonopoulou, D. (1999). Occupation horizons found in the search for the ancient Greek city of Helike. Geoarchaeology, 14, 531–563.

Soter, S., Blackwelder, P.L., Tziavos, C., Katsonopoulou, D., Hood, T., & Alvarez-Zarikian, C. (2001). Environmental analysis of cores from the Helike Delta, Gulf of Corinth, Greece. Journal of Coastal Research, 17, 95–106.

Stanley, D.J., & Hait, A.K. (2000). Deltas, radiocarbon dating, and measurements of sediment storage and subsidence. Geology, 28, 295–298.

Stanley, D.J., & Warne, A.G. (1994). Worldwide initiation of Holocene marine deltas by deceleration of sea-level rise. Science, 265, 228–231.

Stewart, I., & Vita-Finzi, C. (1996). Coastal uplift on active normal faults: The Eliki Fault, Greece. Geophysical Research Letters, 23, 1853–1856.

Stiros, S.C. (1998). Archaeological evidence for unusually rapid Holocene uplift rates in an active normal faulting terrain: Roman harbor of Aigeira, Gulf of Corinth, Greece. Geoarchaeology, 13, 731–741.

Stiros, S.C., & Pirazzoli, P. (1998). Late Quaternary coastal changes in the Gulf of Corinth: Tectonics, earthquakes and archaeology. Gulf of Corinth Field Trip, Guide Book. Geodesy Laboratory, University of Patras.

Stiros, S., Pirazzoli, P., Rothaus, R., Papageorgiou, S., Laborel, J., & Arnold, M. (1996). On the date of construction of Lechaion, western harbor of ancient Corinth, Greece. Geoarchaeology, 11, 251–263.
Tartaron, T.F., Rothaus, R.M., & Pullen, D.J. (2003). Searching for prehistoric Aegean harbors with GIS, geomorphology, and archaeology. Athena Review, 3, 27–36.
Tsokas, G.N., Tsourlos, P., Stampolidis, A., Katsonopoulou, D., & Soter, S. (2009). Tracing a major Roman road in the area of ancient Helike by resistivity tomography. Archaeological Prospection, 16, 251–266.
Wells, D.L., & Coppersmith, K.J. (1994). New empirical relationships among magnitude, rupture length, rupture width, rupture area, and surface displacement. Bulletin of the Seismological Society of America, 84, 974–1002.

Received 28 March 2010
Accepted for publication 11 March 2011
Scientific editing by Jeff Blackford